Gripper Point Contacts for Part Alignment

Mike Tao Zhang, *Member, IEEE*, and Ken Goldberg, *Senior Member, IEEE*

 Abstract — The initial resting pose of many industrial parts differs from the orientation desired for assembly. We show that it is possible to align parts during grasping using a standard parallel-jaw gripper. A solution is an arrangement of four gripper point contacts that will align the part in the vertical plane as the jaws close. Given a *n*-sided polygonal part and *k* uniformly distributed sample points on each side, we present an $O(n^4 k^4)$ numerical algorithm to compute a set of solutions or a report that no solution exists. The algorithm combines toppling, accessibility, and form-closure analysis. We have implemented the algorithm and report sensitivity data from physical experiments.

Index Terms — Robot grasping, toppling manipulation, gripper design, part feeding.

I. INTRODUCTION

"Grippers can be the most design-intensive components of an assembly system" [15]. Although grippers are widely used for automated manufacturing, assembly, and packing, designing gripper jaws is usually ad-hoc and remains a limiting factor in industrial applications. This paper proposes a new approach based on mechanics and part geometry.
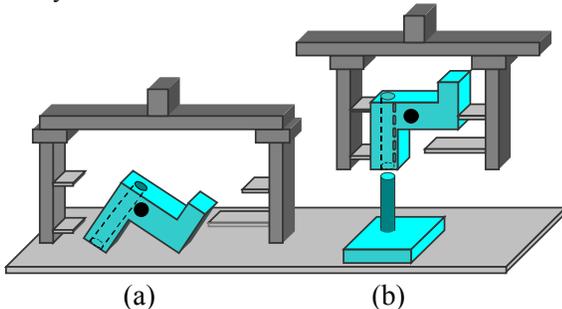
Fig. 1. Gripper contacts align the part for assembly.

Industrial parts on a flat worksurface will naturally come to rest in one of several stable orientations [12], but it is often necessary to rotate parts into different orientations for assembly. Fig. 1 illustrates how parts can be aligned using a standard parallel-jaw gripper. The part is initially in stable orientation (a); as the jaws close, the part is passively rotated into orientation (b) for assembly onto the peg.

Mike Tao Zhang is with Technology and Manufacturing Group, Intel Corporation, 2501 NW 229th Street, Hillsboro, OR 97124, USA. K. Goldberg is with the Department of Industrial Engineering and Operations Research and the Department of Electrical Engineering and Computer Science, University of California, Berkeley, CA 94720 – 1777, USA. For more information, please contact: goldberg@ieor.berkeley.edu.

Given part geometry, we study how to compute the position of four gripper contacts. We illustrate notation in Fig. 2. Pushing tip *A'* and toppling tip *A* make contact with the part to rotate it from the initial stable orientation to its desired orientation, and then fixturing tips *B'* and *B* make contact with the part, stop its rotation, and securely grasp it. The gripper with four jaw tips is low in cost, footprint, and weight, and can be rapidly reconfigured to handle different parts.
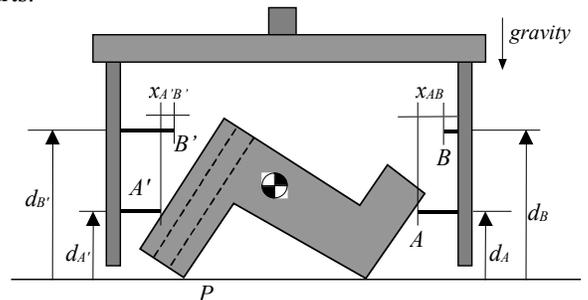
Fig. 2. Contacts *A* and *A'* rotate the part into its desired orientation. It is then grasped with contacts *B* and *B'*.

II. RELATED WORK

There is a substantial body of research on robotic grasping. Useful surveys can be found in [13], [24], [16], [26], [34], [27], [3], and [4].

Final grasp configurations can be analyzed with classical screw theory. Markenscoff *et al.* [21] prove, by infinitesimal perturbation analysis, that four (seven) hard contacts are necessary and sufficient to achieve form closure of a 2D (3D) object in the absence of friction. Trinkle [39] presents a quantitative test for form closure grasps in term of linear programming. Ponce *et al.* [28] address the problem of stable grasps of 3D parts and derive necessary and sufficient conditions for equilibrium and force-closure. Rimon and Burdick [33] provide exact decision process for immobilization based on higher order derivatives of part motion in C-space. Han *et al.* [14] formulate grasping problems as a set of convex optimization problems involving linear matrix inequalities. Liu [18] presents an $O(n^{3n/2})$ algorithm to compute all *n*-contact form closure grasps on a polygonal object.

A number of papers consider part motion in the horizontal plane. The motion of parts during grasp acquisition is analyzed by Mason [22], who studies push mechanics as a role of passive compliance in grasping and manipulation. Erdmann and Mason [9] explore the use of motion strategies to reduce uncertainty in the location of objects. They describe a systematic algorithm for sensorless manipulation to orient parts using a tilting tray. Brost [6] analyzes the mechanics of the parallel-jaw gripper showing

that it is possible to align parts using passive pushes and squeeze mechanics. Goldberg [11] proves that a modified parallel-jaw gripper can orient any polygon up to symmetry by a sequence of normal pushes. Akella *et al.* [2] introduce a minimalist manipulation method to feed planar parts using a one-joint robot over a conveyor belt. Qiao and her colleagues apply the concept of attractive regions to peg-in-hole insertion operations [29] and to pushing and grasping in 3D C-spaces [30].

Several authors address motion of parts in the vertical (gravitational) plane during grasping. Erdmann [10] studies nonprehensile manipulation in C-space and develops an algorithm for sensorless part orienting. Abell and Erdmann [1] study how a planar polygon can be rotated while stably supported by two frictionless contacts. Zumel and Erdmann [46][47] analyze nonprehensile manipulation using two palms jointed at a central hinge. Rao *et al.* [31] give an analysis for picking up polyhedral parts using 2 hard-point contacts with a pivoting bearing, allowing the part to pivot under gravity to rotate into a new configuration. Blind *et al.* [5] present a "*Pachinko*"-like device to orient polygonal parts in the vertical plane. It consists of a grid of retractable pins that are programmed to bring the part to a desired orientation as the part falls. Moll and Erdmann [25] orient parts by dropping them on specially designed surfaces. They adjust the shape of the surface and the drop height to obtain a combination that yields a minimal entropy distribution of the part's final orientation.

Perhaps closest to the current paper, which addresses multiple-contact toppling and grasping, is the work of Trinkle *et al.* [37][38], which analyzes lifting parts off a work-surface using a planar gripper with two pivoting jaws. They generate *liftability regions* corresponding to the contacts causing the object to: slide, jam, break either of two contacts with the surface, or break both contacts with the surface. One important difference is that we focus on part alignment using only translational motion of gripper jaws. Kaneko *et al.* [17] derive a sufficient condition to move an enveloped part using a set of torque commands. To efficiently predict the dynamic behavior of a grasp, Song *et al.* [36] provide a hybrid approach by switching to a compliant model when a rigid body model has no unique solution.

Wallack and Canny [40] develop an algorithm for planning planar grasp configurations using a modular vise. Brown and Brost [7] turn the vise upside down to form a modular parallel-jaw gripper. Each jaw consists of a regular grid of precisely positioned holes. By properly locating (inserting) four pins on each grid, the object can be grasped reliably in the desired orientation. They give an efficient algorithm for computing optimal positions for pins depending on a planar fixture model and additional 3-D geometry analysis.

Our work is also motivated by recent research in toppling manipulation. Zhang and Gupta [42] study how parts can be reoriented as they fall down a series of steps. The authors derive the condition for toppling over a step and defined the transition height, which is the minimum step height to topple a part from a given stable orientation to another. Yu *et al.* [41] estimate the center of mass

(COM) of objects by toppling. Lynch [19] [20] derives sufficient mechanical conditions for toppling parts on a conveyor belt in term of constraints on contact friction, location, and motion. For pin design, we introduce a set of geometric functions to describe the mechanical property of toppling [43].

The approach described in this paper is consistent with the guidelines proposed by Causey and Quinn [8] for the design of grippers for manufacturing: include functionality in gripper jaws, use jaws to align parts, and design for proper gripper-part interaction. We combine toppling mechanics with an analysis of jamming, accessibility, and form closure in the gravitational plane. A preliminary report on this approach appeared in [44].

III. PROBLEM DEFINITION

Given a part, we want four contacts that will rotate it into a desired orientation and grasp it securely. The input is: the vertices of an n-sided convex projection of an extruded polygonal part, its center of mass (COM), initial and desired orientations, a vertex clearance radius ε, and bounds on the part-surface friction coefficient $[0, \mu_{s\_max}]$ and on the part-gripper friction coefficient: $[\mu_{t\_min}, \mu_{t\_max}]$. The output of the algorithm is a report that no solution can be found or a set of solutions, each given as the position of four jaw tips (see Fig. 2).
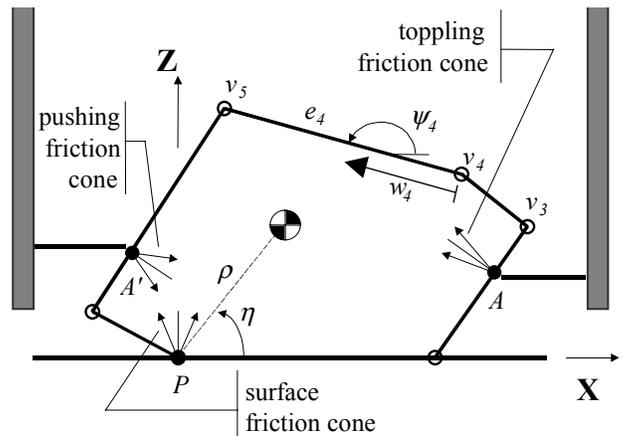
Fig. 3. Convex hull of the part in Fig. 2.

Fig. 3 shows the convex hull of the part sitting on a flat work-surface in its stable orientation. We define a frame originating at P with X-axis on the surface pointing right and Z-axis pointing up. This frame translates to the right as the part is pushed.

Consider the part at its initial orientation. Its COM is a distance ρ from P and an angle η from the +X direction. Starting from P, we consider each edge of the part in counter-clockwise order: $e_1, e_2, \ldots, e_n$. The edge e_i, with vertices v_i at (x_i, z_i) and v_{i+1} at (x_{i+1}, z_{i+1}), is in direction ψ_i from the +X axis. Let w_i be the distance along edge e_i as shown in Fig. 3. Any point on e_i can be expressed as $(x_i + w_i \cos\psi_i, z_i + w_i \sin\psi_i)$.

Let θ denote the rotational angle of the part as measured from the X-axis. Initially $\theta = 0$; θ_d is the part's

desired orientation and θ_l is its next stable orientation in the counter-clockwise direction. We assume $\theta_d < \theta_l$. We say an edge e_k is *visible* if it can be seen from +X direction; *invisible*, otherwise. Thus, e_k is visible if $0 < \psi_k + \theta < \pi$; e_k is invisible if $\pi < \psi_k + \theta < 2\pi$. Note that A can only make contact with visible edges and that A' can only make contact with invisible edges.

Our analysis involves the graphical construction of a set of geometric functions that represent the mechanics of part alignment including the vertex function and the rolling function. These functions are dependent on θ and map from part orientation to height: $S^1 \to \mathfrak{R}^+$, where S^1 is the set of planar orientations.

We assume that the part and the gripper are rigid, and that the part's geometry, the location of its COM, and the position of the jaws are known exactly. We also assume that inertial effects are negligible during part motion. Without loss of generality, we assume that the part will be rotated counter-clockwise. Jaw tips for clockwise rotation can be computed using a mirror image of the part.

IV. TOPPLING

Toppling tip A and pushing tip A' make contact with the part and rotate it counterclockwise during toppling. The part maintains contact with the work-surface at pivot point P. We assume the toppling tip A' keeps contact with edge e_n in this paper (see [45] for general cases).
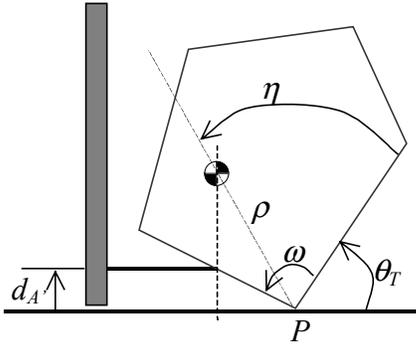
Fig. 4. θ_T: critical angle where part is going to rotate about A' and lose contact with P.

The part is rotated from initial orientation $\theta = 0$ to the desired orientation θ_d. Let θ_T denote the critical rotational angle where the COM is directly above A'. Let ω denote the interior angle of the part at pivot point P. As shown in Fig. 4, we have:

$$d_{A'} / \tan(\theta_T + \omega) = \rho \cos(\eta + \theta_T). \quad (1)$$

Thus the desired orientation of the part must be within the range $\theta_d \in [0, \theta_T]$, otherwise the part will rotate about A' and lose contact with P.

Let θ_C denote the critical transition angle where the COM is directly above P. We divide toppling into two phases: *rolling* and *settling*, where $0 < \theta < \theta_C$ and $\theta > \theta_C$ respectively.

The radius function, $R(\theta)$, is the height of the COM as the part is rotated [22]. The local minima of the radius

function correspond to stable orientations of the part; the local maxima correspond to the critical angle θ_C's. Each vertex of the part defines a vertex function, $V_i(\theta)$, which gives the height of vertex i as the part rotates. The vertex functions define which part edge a jaw tip at a given height will touch. Given $d_{A'}$, the range of friction coefficients, and the toppling tip A in contact with edge e_i, the rolling function $H_i(\theta)$ is the minimum height of A guaranteed to cause the part to rotate at orientation θ.

We assume that part-worksurface and part-gripper friction coefficients μ_s and μ_t (their corresponding friction cone half-angles are $\alpha_s = \tan^{-1}\mu_s$ and $\alpha_t = \tan^{-1}\mu_t$ respectively) are given precisely in section A and B. We then relax this assumption to define $H_i(\theta)$ given bounds on μ_s and μ_t.

A. Rolling Phase

During the rolling phase, the part has three contacts at A', A, and P with corresponding pushing, toppling, and surface friction cone as shown in Fig. 5. The part rotates and translates relative to these contacts. The system of forces on the part, including the contact force at the work-surface, the contact force at the tips, and the part's weight, must generate a counterclockwise moment on the part with respect to pivot point P. The contact force at P is along the left edge of the surface friction cone, but the direction of the contact force at A' depends on angle $\omega + \theta$.

Consider the case where $\pi > \omega + \theta > \pi/2$. Rotation causes the contact between the part and A' to move away from P. Thus the contact force at A' is along the left edge of the pushing friction cone.

We use a graphical method, "moment labeling", to find the rolling function. This method was first presented by Reuleaux [32]. Mason [23] applied it to study multiple planar contact problems. Van der Stappen *et al.* [35] gave a polynomial-time algorithm to compute all form closure grasps on a polygonal part using this method.
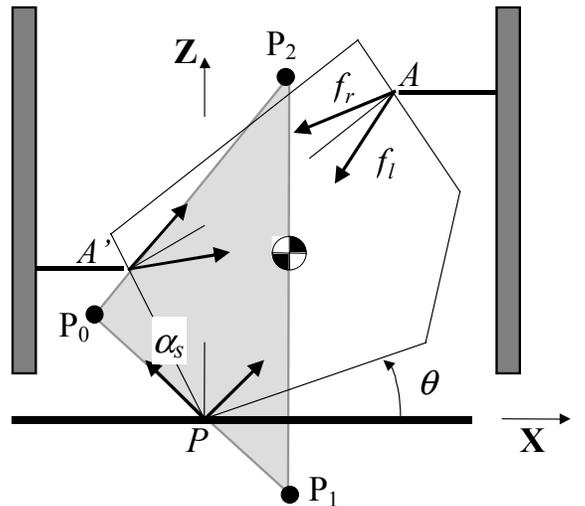
Fig. 5. Rolling phase ($\pi > \omega + \theta > \pi/2$): the part maintains contact with A', A, and P. Vectors at each contact represent the left and right edges of the corresponding friction cones.

We construct a triangle $P_0P_1P_2$ as shown in Fig. 5. Each edge of the triangle corresponds to a contact force or gravity force. P_0 is at (x_{p0}, z_{p0}), which is the intersection of the left edge of the surface friction cone and the left edge of the pushing friction cone. P_1 is at (x_{p1}, z_{p1}), which is the intersection of the vertical line through the COM and the left edge of the surface friction cone. P_2 is at (x_{p2}, z_{p2}), which is the intersection of the vertical line through the COM and the left edge of the pushing friction cone. Let r_{01} denote the line segment between P_0 and P_1 and let $|r_{01}|$ denote its length. We denote r_{02}, r_{12}, $|r_{02}|$, and $|r_{12}|$ similarly. Thus we have:

$$x_{p0} = t - |r_{01}|\sin\alpha_s, \tag{2}$$
$$z_{p0} = -t/\mu_s + |r_{01}|\cos\alpha_s, \tag{3}$$
$$x_{p1} = t, \tag{4}$$
$$z_{p1} = -t/\mu_s, \tag{5}$$
$$x_{p2} = t, \tag{6}$$
$$z_{p2} = \frac{\dfrac{d_{A'}}{\tan\varphi} - t}{\tan(\varphi + \alpha_t)} + d_{A'}, \tag{7}$$

where $t = \rho\cos(\eta + \theta)$, $\varphi = \omega + \theta$ and $\tag{8}$

$$|r_{01}| = \frac{(z_{p2} + \dfrac{t}{\mu_s})\sin(\varphi + \alpha_t)}{\sin(\varphi + \alpha_t - \alpha_s)}. \tag{9}$$

The locations of P_0, P_1, and P_2 are a function of θ. As θ increases, P_1 shrinks to P along r_{01}, r_{02} sweeps counterclockwise, and P_2 moves up while r_{12} remains parallel to the Z-axis. Triangle $P_0P_1P_2$ exists if and only if $\omega + \theta + \alpha_t < \pi$, i.e. $\theta < \pi - \omega - \alpha_t$.

If every force in the toppling friction cone makes a positive moment about every point in the $P_0P_1P_2$ triangle, the only part motion possible is rotation about P as the jaws are closed. For all forces in the toppling friction cone to generate a counterclockwise moment about the triangle, the left edge of the friction cone must pass above the triangle; all other vectors in the friction cone will pass higher. We denote the vector at the left edge of the toppling friction cone as f_l and the right edge as f_r. We find the height of A sufficient to roll the part by projecting lines from P_0, P_1, and P_2 along angle f_l into the edge contacting A. The maximum of these projections is the minimum height of A sufficient to roll the part. Note that this is also the minimum height of A to keep the part on the worksurface.

Let $w_{i,2}$ denote the distance from vertex v_i to A along edge e_i where the left edge of the toppling friction cone passes exactly through point P_2. Let X_i and Z_i denote the location of vertex v_i after the part undergoes pure rotation by angle θ, i.e., $X_i = x_i\cos\theta - z_i\sin\theta$ and $Z_i = x_i\sin\theta + z_i\cos\theta$. We can show through geometric construction that:

$$w_{i,2}(\theta) = \frac{Z_i - z_{p2} - (X_i - x_{p2})\tan\gamma_{il}}{\cos\xi_i\tan\gamma_{il} - \sin\xi_i} \tag{10}$$

where $\xi_i = \theta + \psi_i$ and $\gamma_{il} = \theta + \psi_i + \alpha_t + \pi/2$.

The distances $w_{i,0}$ and $w_{i,1}$ are defined similarly, where the left edge of the toppling friction cone intersects P_0 and P_1 respectively.

The rolling function, $H_i(\theta)$, is based on $w_i(\theta)$ that is max $(w_{i,0}(\theta), w_{i,1}(\theta), w_{i,2}(\theta))$. $w_i(\theta)$ can be shown to be:

$$w_i = \begin{cases} w_{i,2} & 0 < \theta < \theta_m \text{ and } \psi_i < \omega \\ w_{i,0} & 0 < \theta < \theta_m \text{ and } \psi_i \geq \omega, \\ \infty & \text{otherwise} \end{cases} \tag{11}$$

where $\theta_m = \min(\theta_C, \pi - \omega - \alpha_t)$. Thus, the rolling function is given by:

$$H_i(\theta) = \begin{cases} H_i^*(\theta) & V_i(\theta) \leq H_i^*(\theta) \\ 0 & V_i(\theta) > H_i^*(\theta) \end{cases}, \tag{12}$$

where $H_i^*(\theta) = Z_i + w_i\sin\xi_i$. $\tag{13}$

Following the same methodology, we find $H_i(\theta)$ under the condition $\pi/2 > \omega + \theta > 0$.
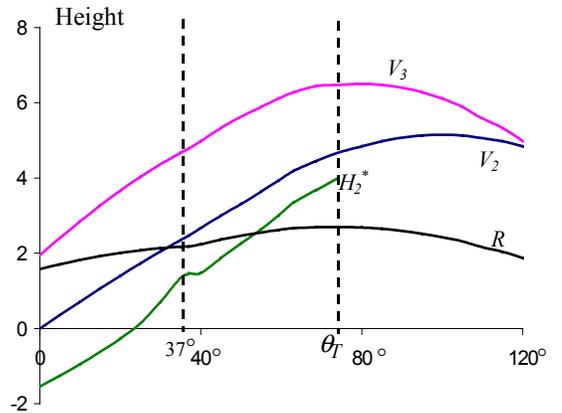
Fig. 6. Vertex functions and rolling function.

Fig. 6 illustrates function $R(\theta)$, $H_2^*(\theta)$, $V_2(\theta)$ and $V_3(\theta)$ for the part in Fig. 3 with $\alpha_t = 5°$, $\alpha_s = 10°$ and $d_{A'} = 9$. The kink ($\theta = 37°$) of $R(\theta)$ represents the orientation where e_6 is on the surface. At a certain angle θ, any A at height h will instantaneously rotate the part if max $(H_2(\theta), V_2(\theta)) < h < V_3(\theta)$. The toppling function indicates that A can roll the part at any contact on e_2 when $0 < \theta < 20°$.

B. Settling Phase

If the desired final orientation of the part θ_d is greater than θ_C, the part will enter the settling phase. It is important to guarantee that the part remains in contact with A, A', and the worksurface. Since the part rotates counterclockwise, the contact force at A' is in the direction of the left edge of the pushing friction cone and the contact force at P is in the direction of the left edge of the surface friction cone.

We now define another critical angle, θ_E, beyond which the part may accelerate under gravity and lose contact with A. To avoid this, we require that $\theta_d < \theta_E$.
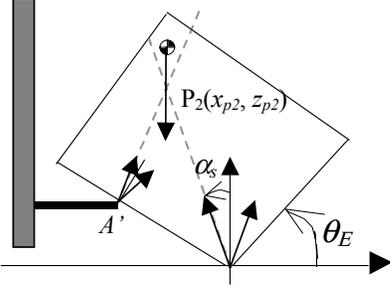
Fig. 7. θ_E: critical angle where sliding starts.

To solve for θ_E we find the critical angle at which the part remains stationary with only contacts at A' and P. This corresponds to the angle where P_2 is on the left edge of the surface friction cone, i.e., the vertical line through the COM, the left edge of the surface friction cone and the left edge of the pushing friction cone intersects at the same point. As shown in Fig. 7, $\tan\alpha_s = |\,x_{p2}/z_{p2}\,|$. Therefore, we have the following equation to solve for θ_E:

$$[d_{A'} + \rho \tan\alpha_s \cos(\eta+\theta_E)] \tan(\omega+\theta_E) \tan(\omega +\theta_E+\alpha_t) - \rho \cos(\eta+\theta_E) \tan(\omega+\theta_E) + d_{A'} = 0. \quad (14)$$

To find the minimal height of the toppling tip that is guaranteed to roll the part, we construct the triangle $P_0P_1P_2$ (see Fig. 8) and compute the rolling function as described in the last section.
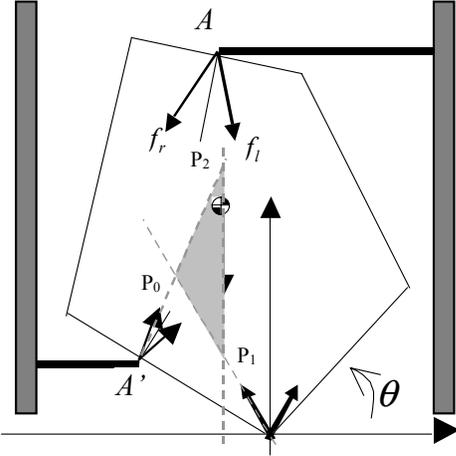
Fig. 8. Settling phase.

C. Bounded Friction Coefficients

In the previous section we assumed exact friction values were given. In this section we relax that assumption and derive the rolling function given upper and lower *bounds* on the friction coefficients.

For each value of θ, the geometric functions can take on a range of values depending on the range of friction coefficients. To guarantee toppling for all the friction values in the range, we take the maximum values of

$H_i(\theta)$ over the given bounds. At each rotational angle θ, the maximum $H_i(\theta)$ corresponds to the *critical friction coefficients* denoted by $\mu_s^*(\theta)$ and $\mu_t^*(\theta)$. We first consider the function at each rotational angle θ to derive $\mu_s^*(\theta)$; then we find $\mu_t^*(\theta)$ for given $\mu_s^*(\theta)$ and θ.

As illustrated in Fig. 5, during rolling, P_0 moves up along r_{02} as μ_s decreases. Then, $w_{i,0}$ decreases while $w_{i,2}$ remains unchanged. Therefore $H_i(\theta)$ is guaranteed not to increase as μ_s decreases. It is sufficient to consider only the upper bounds of μ_s, i.e. $\mu_s^*(\theta) = \mu_{s\_max}$, to get the maximal $H_i(\theta)$ over the given range of μ_s.

Given θ and $\mu_s^*(\theta) = \mu_{s\_max}$, the rolling function is a function of μ_t. In Fig. 5, P_2 moves down along r_{12} as μ_t decreases. Therefore, $w_{i,2}$ decreases and $\mu_t^*(\theta) = \mu_{t\_max}$ if w_i is determined by $w_{i,2}$. But P_0 moves up along r_{01} as μ_t decreases, so $\mu_t^*(\theta) = \mu_{t\_min}$ if w_i is determined by $w_{i,0}$.

As illustrated in Fig. 8, during settling, P_0 moves up along r_{02} and P_1 moves up along r_{12} as μ_s decreases. So $\mu_s^*(\theta) = \mu_{s\_max}$. P_2 moves down along r_{12} and P_0 moves down along r_{01} as μ_t decreases. Thus $\mu_t^*(\theta) = \mu_{t\_max}$.

In summary, we find $H_i(\theta)$ over the range of μ_s and μ_t by determining $\mu_s^*(\theta)$ and $\mu_t^*(\theta)$ at each θ, where $\mu_s^*(\theta) = \mu_{s\_max}$ in both rolling and settling phase and $\mu_t^*(\theta) = \mu_{t\_max}$ in settling phase. For $\mu_t^*(\theta)$ in rolling phase, it is shown to be μ_{t_min} if $\psi_i > \omega$ and μ_{t_max} if $\psi_i < \omega$.

D. Toppling Function

The toppling function is a vector function that combines the vertex functions and the rolling functions for the visible edges over the range $\theta \in [0, \min(\theta_T, \theta_E)]$. The rolling functions correspond to $\mu_s^*(\theta)$ and $\mu_t^*(\theta)$. From the toppling function, we can either determine or show to be non-existent the range of toppling tip heights that are capable of rotating the part to the desired orientation.
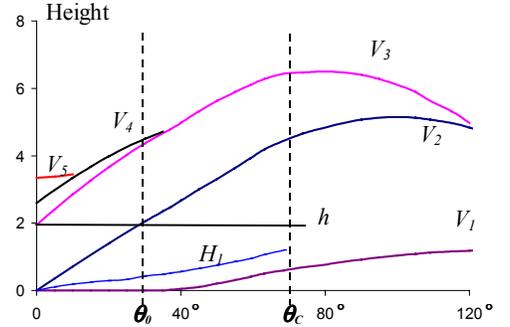
Fig. 9. Toppling function.

Fig. 9 illustrates the toppling function for the part in Fig. 5. We consider the toppling tip at height h (shown as height = 2 in the figure). θ_0 is the rotational angle where h intersects V_2, where contact A will move from edge e_2 to e_1. θ_C is the critical angle where the center of mass is exactly above the pivot point. H_1 is the rolling function, which gives the minimum height of A that is in contact with e_1. H_1 is bounded by V_1 and V_2 and is truncated where it intersects them. H_2 is 0 in the range $\theta \in [0, \theta_0]$. Since h is above H_1

and H_2, a toppling tip at height h will rotate the part from a stable initial orientation with $\theta = 0$ to $\theta = \theta_C = 71°$.

A toppling tip at height h will achieve this if we can draw a horizontal line corresponding to height h in the toppling function beginning at $\theta = 0$ and ending at θ_d with the following characteristics:

$$1: h > H_i(\theta), \text{ if } V_i(\theta) < h < V_{i+1}(\theta); \qquad (15)$$
$$2: h < \max_i (V_i(\theta)), \text{ if } \theta < \theta_C. \qquad (16)$$

where i is the index for the visible edges.

The first criteria are satisfied when the toppling tip is above the rolling function of the edge it contacts. When h crosses a vertex function, the part switches contact edges and then h must be above the rolling function for the new edge. The second criterion is that the toppling tip must not lose contact with the part by passing over it during the rolling phase.

From the toppling function we can determine that the toppling tip at $d_{A'} = h = 2$ will topple the part to θ_C.

V. ACCESSIBILITY

During toppling, the part is constrained by three contacts: the toppling tip A, the pushing tip A' and the pivot point P on the work-surface. Once the part has been rotated to the desired orientation θ_d, the fixturing tips, B and B', must terminate its rotation and achieve a form closure grasp with A and A'.

The accessibility constraint insures that B and B' do not collide with the part before it reaches its desired orientation. It will limit the possible heights of B and B' for given $d_{A'}$ and d_A.
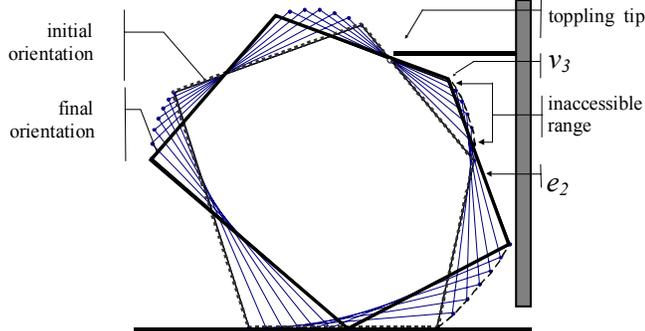
Fig. 10. Rotation of a part relative to the toppling tip A. Dotted/solid lines indicate the initial/final orientation of the part and dashed lines represents the motion trajectory of vertices.

To insure accessibility from B, the point on the part at height d_B can only move towards tip B. A similar condition applies for fixturing tip B'. The *inaccessible range* shown in Fig. 10 indicates heights of B that would collide with the part before its desired orientation.

To compute the inaccessible range for B, we note that as the part rotates, the horizontal velocity of points on the part edges relative to tip A can be positive, negative and zero. There may be a point on each visible edge that has zero velocity as the part rotates through angle θ. Let B_θ be this point on edge e_j and h_θ be its height. Below h_θ, the

relative velocity of the points on e_j is positive and B_θ moves towards tip B; above h_θ, the relative velocity is negative and B_θ moves away from tip B. The accessibility constraint requires $d_B \leq h_\theta$ for all visible edges at all θ.

To solve for h_θ, we derive an expression for the horizontal distance between A and B_θ using the fact that the part is constrained by A and P:

$$x_\theta = X_j - X_i + \frac{d_B - Z_j}{\tan \xi_j} - \frac{d_A - Z_i}{\tan \xi_i}, \qquad (17)$$

where i and j are the indexes of the edges in contact with A and B respectively and $\xi_i = \theta + \psi_i$ as defined in Equation (10). To find the point with zero horizontal velocity relative to tip A, we take the derivative of x_θ with respect to θ:

$$\frac{dx_\theta}{d\theta} = Y_i - \frac{d_A - X_i}{\tan \xi_i} + \frac{d_A - Y_i}{\sin^2 \xi_j} - Y_j + \frac{d_B - X_j}{\tan \xi_j} - \frac{d_B - Y_j}{\sin^2 \xi_j}. \quad (18)$$

We set (18) equal to 0, and then solve for d_B to yield:

$$h_\theta = d_B = \frac{\left[Y_i - \frac{d_A - X_i}{\tan \xi_i} + \frac{d_A - Y_i}{\sin^2 \xi_j} - Y_j \right] - \frac{X_j}{\tan \xi_j} + \frac{Y_j}{\sin^2 \xi_j}}{\left[\frac{1}{\tan \xi_j} - \frac{1}{\sin^2 \xi_j} \right]} \qquad (19)$$

For a given visible edge, we consider heights less than h_θ for the fixturing tip B.

Accessibility constraints for B' on the part's the invisible edges can be obtained similarly. Given d_B, $d_{B'}$ and the final orientation of the part, we can then compute the offset between tips along +X-axis (see x_{AB} and $x_{A'B}$ in Fig. 2) to get the location of the fixturing tips.

VI. FORM-CLOSURE

We also require that the set of four tip contacts generate a form closure grasp. We construct a 3×4 wrench matrix **W** based upon the X (Z)-axis projection and the torque of the unit normal inward vectors at the contacts. Let **λ** denote a 4×1 vector. The four contacts achieves a form closure grasp if and only if $\exists$ **λ** > 0, s.t. **Wλ** = **0**. Given **W**, we can determine whether there exists such a **λ** in time $O(1)$. We compute the 3×3 minors **W**$_i$ obtained by removing the ith column from **W**. There exists a **λ** > 0 satisfying **Wλ** = **0** if all the minors **W**$_i$ have the same sign and none of them is zero [40]. The four tips achieve a form closure grasp on the part if this condition is satisfied.

VII. ALGORITHM COMPLEXITY

We give a polynomial-time numerical algorithm to solve the gripper contact problem. An asymptotic upper bound of its running time can be derived as follows.

Given an *n*-sided polygonal part, we sample its invisible edges to obtain the height of the pushing tip, $d_{A'}$, and sample its visible edges to obtain the height of the pushing tip, d_A. Let k be the number of uniformly distributed sample points on each edge.

For each $d_{A'}$, we construct the corresponding toppling function. It takes $O(1)$ time to compute each geometric function for a visible edge. There are $O(n)$ visible edges in a graph, so the time to compute each toppling function is $O(n)$. The toppling function allows us to identify in time $O(n)$ if a toppling tip at height d_A can rotate the part to the desired orientation with the given $d_{A'}$. So it takes time $O(n)+O(kn)O(n)$ to find all the feasible d_A for each $d_{A'}$. Therefore, the running time to find all the feasible $(d_A, d_{A'})$ pairs is $O(k^2n^3)$.

Given a pair of feasible $(d_A, d_{A'})$, we apply an $O(n)$ time accessibility analysis to generate the accessible ranges for the fixturing tips. We can then identify the fixturing tips within the accessible ranges in time $O(kn)$. Next we check if each four-contact set achieves form-closure in time $O(1)$. Since there are $O(k^2n^2)$ feasible pairs of $(d_A, d_{A'})$ and there are $O(kn)$ left and right fixturing tips with in the accessible ranges respectively, the algorithm takes time $O(k^4n^4)$ to find the solution or to show no solution exists.

VIII. IMPLEMENTATION AND EXPERIMENTS

We implemented our jaw contact design algorithm as an application using the Java programming language. Mouse input allows a user to draw a part, define its COM and friction, and select its initial and final orientations; the program then computes and displays the resulting solutions or reports that no solution exists.
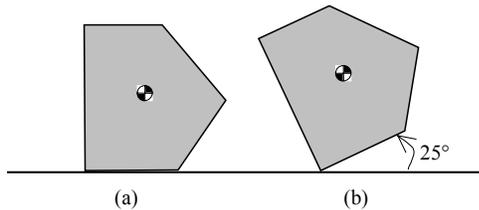
Fig. 11. An example: part alignment.

An example is illustrated in Fig. 11. The part is defined by the vertices at (0,0), (51.2, 0), (64.1, 57.2), (37.5, 96.2), (-32.2, 44.6), and COM at (21.9, 42.3). It is initially in stable orientation (a) and we desire to rotate it 25º into final orientation (b) for assembly.
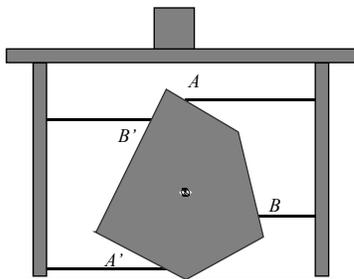
Fig. 12. A resulting jaw design to align the sample part.

Fig. 12 illustrates a computed jaw design for the sample part, where A at (5.93, 95.61), A' at (-6.17, 4.55), B at (42.05, 31.83), and B' at (-21.53, 78.02).

Fig. 13. Experimental workcell: the robot picks up parts from a convey belt using the parallel-jaw gripper.

To explore robustness to initial conditions, we conducted physical experiments using an *AdeptOne* industrial robot and a pneumatic parallel-jaw gripper (*Mecanotron* serial number: 101167) as shown in Fig. 13. The gripper jaws were designed by the algorithm and manually assembled from aluminum stock. To control the velocity of our pneumatic gripper, we added two air regulators (*Wilkerson* serial number: R08-01-F000) and two compression springs (*Century* serial number: C-606).
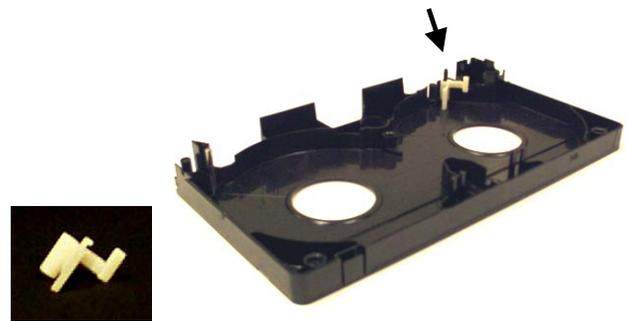
Fig. 14. Natural resting pose of the lever and the assembly: the lever (in white) inserted onto the vertical post.

The part we used is a small lever from a commercial videotape cassette (*Fuji* serial number: 7410161160). As shown in Fig. 14, the lever must be rotated from the natural resting pose and inserted into a vertical post on the videotape cassette. Its planar convex hull is shown in Fig. 3. The COM and friction coefficients were determined by physical experiments.

Fig. 15 illustrates a successful grasp where the lever rotates in the vertical plane from its resting pose to the desired orientation $\theta_d = 37°$. The part begins in stable orientation in (1). Its desired orientation for insertion is (5). We choose A and A' at $d_A = 6$mm and $d_{A'} = 5$mm,

respectively. The friction cone bounds are $\alpha_t = [0, 5°]$ and $\alpha_s = [0, 10°]$. $x_2 = 14$mm, $z_2 = 0$mm, $\psi_2 = 56°$, $\eta = 46°$, $\rho = 7$mm, and $\omega = 53°$. For $k = 10$, the algorithm requires approximately one second on a 233MHz Pentium II PC running Microsoft J++ 6.0 to find 43 solutions. The gripper jaws in Fig. 15 have the following contact values: $d_B = 11$mm, $d_{B'} = 13$mm, $x_{AB} = 5$mm, and $x_{A'B'} = 1$mm.
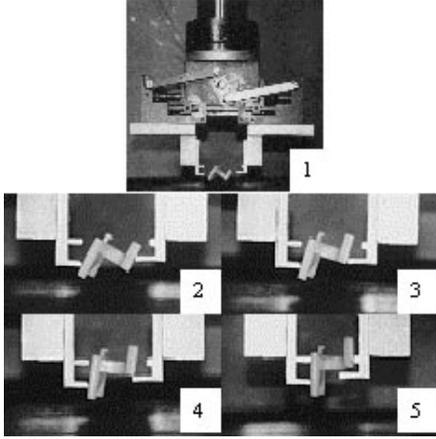
Fig. 15. Part aligning experiment.

We conducted two experiments to test sensitivity. In Experiment 1, we tested the gripper 50 times at each of seven height offsets. The results are shown in Fig. 16. All 50 trials were successful at the nominal gripper height (offset = 0). But grasping is sensitive to small variations in gripper height; the part can jam in the gripper or be ejected when the gripper height is offset.
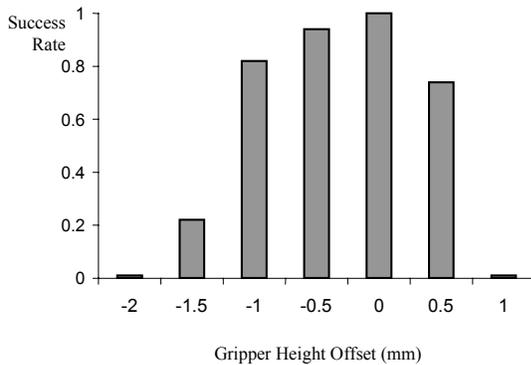
Fig. 16. Success rate when the height of the gripper varies.

In Experiment 2, we vary gripper angle. Fig. 17 illustrates a top view of the part (in gray) and the gripper jaws (in black). The arrows indicate the motion direction of jaws: δ is the angular error.
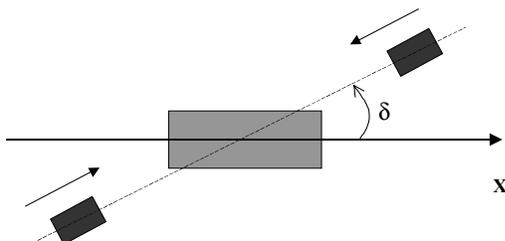
Fig.17. Top view: Error in gripper angle δ.

Fig. 18 shows that all 50 trials are successful even when the gripper is rotated by $\pm 10°$. Grasping can fail for larger rotations, where the part is ejected or causes the gripper to jam.
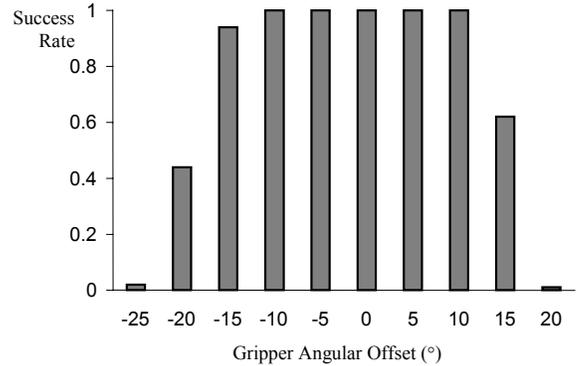
Fig. 18. Success rate when the angle of the gripper varies.

IX. DISCUSSION AND FUTURE WORK

Designing gripper jaws is particularly challenging when the natural resting pose of a part differs from the pose desired for insertion. In this paper we consider a minimalist solution where four contact tips on a parallel-jaw gripper guide the part into alignment and hold it securely. We analyze the gripper contact design problem based on a geometric analysis of the mechanics of toppling, accessibility, and form closure and give a polynomial-time numerical algorithm.

In future work we will extend our analysis to edge contact models. We will consider gripper jaws, based on trapezoidal modules, that maximize contact between the gripper and the part at its desired final orientation. We will also study shape tolerance of the gripper jaws and investigate the conditions under which solutions are guaranteed to exist.

REFERENCES

[1] T. Abell and M. Erdmann, "Stably supported rotations of a planar polygon with two frictionless Contacts," in *Proc. IEEE/RSJ Int. Conf. Intell. Robots Syst.*, Pittsburgh, PA, 1995, pp. 411-8.

[2] S. Akella, W. Huang, K. Lynch, and M. Mason, "Parts feeding on a conveyor with a one joint robot," *Algorithmica*, vol. 26, no. 3-4, pp. 313-44, 2000.

[3] A. Bicchi and V. Kumar, "Robotic grasping and contact: a review," in *Proc. IEEE Int. Conf. Robot. Automat.*, San Francisco, CA, 2000, pp. 348-353.

[4] A. Bicchi, "Hands for dexterous manipulation and robust grasping: a difficult road toward simplicity," *IEEE Trans. Robot. Automat.*, vol. 16, no. 6, pp. 652-62, 2000.

[5] S. Blind, C. McCullough, S. Akella, and J. Ponce, "A reconfigurable parts feeder with an array of pins," in *Proc. IEEE Int. Conf. Robot. Automat.*, San Francisco, CA, 2000, pp. 147-53.

[6] R. Brost, "Automatic grasping planning in the presence of uncertainty," *Int. J. Robot. Automat.*, vol. 7, no. 1, pp. 3-17, 1988.

[7] R. Brown and R. Brost, "A 3-D modular gripper design tool," *IEEE Trans. Robot. Automat.*, vol. 15, no. 1, pp. 174-86, 1999.

[8] G. Causey and R. Quinn, "Gripper design guidelines for modular manufacturing," in *Proc. IEEE Int. Conf. Robot. Automat.*, Leuven, Belgium, 1998, pp. 1453-8.

[9] M. Erdmann and M. Mason, "An exploration of sensorless manipulation," *IEEE J. Robot. Automat.*, vol. 4, no. 4, pp. 369-79, 1988.

[10] M. Erdmann, "An exploration of nonprehensile two-palm manipulation," *Int. J. Robot. Res.*, vol. 17, no. 5, pp. 485-503, 1998.

[11] K. Goldberg, "Orienting polygonal parts without sensors," *Algorithmica*, vol. 10, no. 2, pp. 201-25, 1993. Special Issue on Computational Robotics.

[12] K. Goldberg, B. Mirtich, Y. Zhuang, J. Craig, B. Carlisle, and J. Canny, "Part pose statistics: estimators and experiments," *IEEE Trans. Robot. Automat.*, vol. 15, no. 5, pp. 849-57, 1999.

[13] R. Grupen, T. Henderson, and I. McCammon, "A survey of general-purpose manipulation," *Int. J. Robot. Res.*, vol. 8, no. 1, pp. 38-62, 1989.

[14] L. Han, J. Trinkle, and Z. Li, "Grasp analysis as linear matrix inequality problems," *IEEE Trans. Robot. Automat.*, vol. 16, no. 6, pp. 663-74, 2000.

[15] W. Hessler, "How to build simple, effective pick-and-place devices," *Robot Today*, vol. 9, no. 4, pp. 1-5, 1996.

[16] R. Howe and M. Cutkosky, "Touch sensing for robotic manipulation and recognition," in *Robot. Rev. 2*, Khatib, Ed., Cambridge, MA: MIT Press, 1992.

[17] M. Kaneko, K. Harada, and T. Tsuji, "A sufficient condition for manipulation of envelope family," in *Proc. IEEE Int. Conf. Robot. Automat.*, San Francisco, CA, 2000, pp. 1060-7.

[18] Y. Liu, "Computing *n*-finger form closure grasps on polygonal objects," *Int. J. Robot. Res.*, vol. 19, no. 2, pp. 149-58, 2000.

[19] K. Lynch, "Toppling manipulation," in *Proc. IEEE Int. Conf. Robot. Automat.*, Detroit, MI, 1999, pp. 2551-7.

[20] K. Lynch, "Inexpensive conveyor-based parts feeding," *Assembly Automat.*, vol. 19, no. 3, pp. 209-15, 1999.

[21] X. Markenscoff, L. Ni and C. Papadimitriou, "The geometry of grasping," *Int. J. Robot. Res.*, vol. 9, no. 1, pp. 61-74, 1990.

[22] M. Mason and J. Salisbury, *Robotic Hands and the Mechanics of Manipulation*. Cambridge, MA: MIT Press, 1985.

[23] M. Mason, "Two graphical methods for planar contact problems," in *Proc. IEEE/RSJ Int. Workshop Intell. Robots Syst.*, Osaka, Japan, 1991, pp. 443-8.

[24] B. Mishra, J. Schwartz, and M. Sharir, "On the existence and synthesis of multifinger positive grips," *Algorithmica*, vol. 2, no. 4, pp..541-58, 1987.

[25] M. Moll and M. Erdmann, "Manipulation of pose distributions," in *Algorithmic and Computational Robotics: New Directions*, B. Donald, K. Lynch, and D. Rus, Eds., Natick, MA: A K Peters, 2001, pp. 127-41.

[26] R. Murray, Z. Li, and S. Sastry, *A Mathematical Introduction to Robotic Manipulation*. Boca Raton, FL: CRC, 1994.

[27] A. Okamura, N. Smaby, and M. Cutkosky, "A overview of dexterous manipulation," in *Proc. IEEE Int. Conf. Robot. Automat.*, San Francisco, CA, 2000, pp. 255-62.

[28] J. Ponce, S. Sullivan, A. Sudsang, J.-D. Boissonnat, and J.-P. Merlet, "On computing four-finger equilibrium and force closure grasps of polyhedral objects," *Int. J. Robot. Res.*, vol. 16, no. 1, pp. 11-35, 1997.

[29] H. Qiao and S. Tso, "Three-step precise robotic peg-hole insertion operation with symmetric regular polyhedral objects," *Int. J. Production Res.*, vol. 37, no. 15, pp. 3541-63, 1999.

[30] H. Qiao, "Attractive regions formed by constraints in configuration space," in *Proc. IEEE Int. Conf. Robot. Automat.*, Seoul, Korea, 2001, pp. 1071-8.

[31] A. Rao, D. Kriegman and K. Goldberg, "Complete algorithm for feeding polyhedral parts using pivot grasps," *IEEE Trans. Robot. Automat.*, vol. 12, no. 2, pp. 331-42, 1996.

[32] F. Reuleaux. *The Kinematics of Machinery.* Macmilly and Company (1876); republished by Dover (1963).

[33] E. Rimon and J. Burdick, "Mobility of bodies in contact-part I: a 2nd-order mobility index for multiple-finger grasps," *IEEE Trans. Robot. Automat.*, vol. 14, no. 5, pp. 696-708, 1998.

[34] K. Shimoga, "Robot grasp synthesis algorithms: a survey," *Int. J. Robot. Res.*, vol. 15, no. 3, pp. 230-66, 1996.

[35] A. F. van der Stappen, C. Wentink, and M. Overmars, "Computing immobilizing grasps of polygonal parts," *Int. J. Robot. Res.*, vol. 19, no. 5, pp. 467-79, 2000.

[36] P. Song, M. Yashima, and V. Kumar, "Dynamic simulation for grasping and whole arm manipulation," in *Proc. IEEE Int. Conf. Robot. Automat.*, San Francisco, CA, 2000, pp. 1082-7.

[37] J. Trinkle, J. Abel, and R. Paul, "Enveloping frictionless planar grasping," in *Proc. IEEE Int. Conf. Robot. Automat.*, San Francisco, CA, 1987, pp. 246-51.

[38] J. Trinkle and R. Paul, "Planning for dexterous manipulation with sliding contacts," *Int. J. Robot. Res.*, vol. 9, no. 3, pp. 24-48, 1990.

[39] J. Trinkle, "On the stability and instantaneous velocity of grasped frictionless objects," *IEEE Trans. Robot. Automat.*, vol. 8, no. 5, pp. 560-72, 1992.

[40] A. Wallack and J. Canny, "Planning for modular and hybrid fixtures," *Algorithmica*, vol. 19, pp. 40-60, 1997.

[41] Y. Yu, K. Fukuda, and S. Tsujio, "Estimation of mass and center of mass of graspless and shape-unknown object," in *Proc. IEEE Int. Conf. Robot. Automat.*, Detroit, MI, 1999, pp. 2893-8.

[42] R. Zhang and K. Gupta, "Automatic orienting of polyhedral through step devices," in *Proc. IEEE Int. Conf. Robot. Automat.*, Leuven, Belgium, 1998, pp. 550-6.

[43] M. T. Zhang, K. Goldberg, G. Smith, RP Berretty, and M. Overmars. "Pin design for part feeding," *Robotica*, vol. 19, part 6, pp 695-702, 2001.

[44] M. T. Zhang, G. Smith, and K. Goldberg, "Compensatory grasping with the parallel-jaw gripper," in *Proc. 4th Int. Workshop Algorithmic Foundations of Robot.*, Hanover, NH, 2000, pp. FR27-37.

[45] M. T. Zhang, "Optimal design of self-aligning robot gripper jaws," PhD dissertation, Dept. of Industrial Eng., UC Berkeley, 2001.

[46] N. Zumel and M. Erdmann, "Nonprehensile two palm manipulation with non-equilibrium transitions between stable states," in *Proc. IEEE Int. Conf. Robot. Automat.*, Minneapolis, MN, 1996, pp. 3317-23.

[47] N. Zumel and M. Erdmann, "Nonprehensile manipulation for orienting parts in the plane," in *Proc. IEEE Int. Conf. Robot. Automat.*, Albuquerque, NM, 1997, pp. 2433-9.